Post-Pulse Sodium Spike as a Marker of Cardiac Capture: From Modeling to Clinical Evidence

A.P. RAVAZZI, P. DIOTALLEVI
Division of Cardiology, S. Antonio e Biagio Hospital, Alessandria, Italy

M. SASSARA, S. FICILI
Division of Cardiology, Belcolle Hospital, Viterbo, Italy

J. MEIER, C. MILITELLO
Biotronik GmbH, Erlangen, Germany

L. BRANDOLISIO, R. AUDOGLIO
Biotronik SEDA, Milan T/N, Italy

Summary

A pacemaker that assures myocardial capture through automatic output adjustments would improve patient safety, extend battery life, and expedite follow-up visits. At the upstroke of the action potential, the cell membrane impedance strongly decreases due to opening of the sodium (Na) channels. During this phase, which lasts 2 – 4 ms, the myocardial impedance decreases accordingly. Theoretical models of membrane kinetics show that a brief negative dip in intracardiac impedance is expected soon after captured pacing (within 20 ms). The aim of this preliminary clinical investigation was to verify whether right ventricular capture could be recognized from intracardiac impedance changes that result from the Na channels opening. Six patients implanted with an Inos² CLS pacemaker and low-polarization leads were DDD paced at pulse amplitudes below and above the threshold. Bipolar right ventricular intracardiac impedance was (DC) measured by the pacemaker and downloaded via telemetry into a laptop PC for off-line processing. In all patients, a small (mean 2.9 ± 0.8 Ω) and fast (< 6 ms) intracardiac impedance dip was detected 10 – 18 ms after ventricular capture. This dip was not observed during non-captured events. In conclusion, an ultra-fast (within 20 ms) detection of capture is feasible using an impedance-based method. Since the impedance measurement is minimally affected by polarization artifacts, such a method is expected to work with any lead.

Key Words

Intracardiac impedance, pulse amplitude, right ventricular capture

Introduction

Monitoring the effect of myocardial capture generated by a stimulating pulse allows continuous adaptation of the pulse amplitude to the actual threshold level. Such a feature implemented in a pacemaker would increase patient safety and improve hemodynamic performance by assuring myocardial capture. Moreover, it would extend pacemaker longevity by minimizing energy consumption, and reduce follow-up costs by simplifying the pacing threshold assessment.

Since the 1970s, several methods for automatic pacing output assessment have been utilized. Most of them are based on the analysis of the myocardial-evoked response [1-7]. Such methods are strongly affected by polarization artifacts due to charge latency at the electrode-tissue interface. Much effort has been undertaken to avoid this artifact. Some methods simply apply a blanking time; others limit the system functionality to low polarization leads exclusively or implement active

concepts such as charge balance. In the last five years, some of these methods have been introduced in commercial pacemakers [8-10]. Nevertheless, these methods still lack specificity when dealing with fusion beats. The intracardiac impedance signal has also been investigated as a marker for capture control [11]. This physiologic signal is proportional to the blood volume in the heart and reflects myocardial mechanical activity. A major fault of this method is that, should non-capture occur, it is detected too late during the heart cycle to allow delivery of a full energy backup pulse separate from the vulnerable phase. This is due to electromechanical latency.

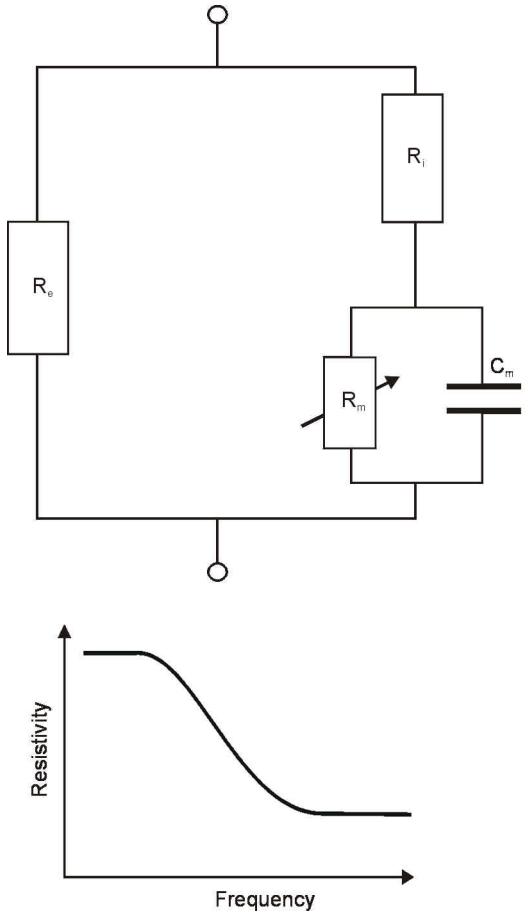

Figure 1. Linear network model of the myocardial tissue. R_e = Resistance of the interstitial space. R_i = Resistance of the intracellular structures/fluids; R_m = Ohmic resistance of the cell membranes; C_m = Membrane capacitance of the cells.

The aim of this study is to evaluate in clinical practice the feasibility of a new concept for fast capture discrimination based on myocardial impedance changes resulting from the opening of sodium channels.

Physiologic Model

The impedance of the myocardial tissue can be modeled as a linear network (Figure 1) [12]. For frequencies up to 10 kHz, the membrane impedance is high and the tissue impedance is mainly set by the interstitial impedance R_e. For higher frequencies the membrane impedance decreases due to its capacitance. At frequencies above 1 MHz the tissue impedance is dominated by R_i ($R_i >> 0.3R_e$). Before and during the myocardial action potential (Figure 2) four phases can be distinguished [13]:

- At rest a transmembrane-potential of -90 mV is maintained by a small but continuous outflow of potassium ions that counteracts the sodium-potassium pump.
- At the initialization of the action potential, there is a fast upstroke of the transmembrane potential due to a short and intense sodium current moving into the cell.
- During the plateau phase the potassium currents slowly increase. The membrane potential is kept at an increased value due to a compensatory inflow of calcium ions.
- The calcium outflow drops to zero and the membrane potential returns to its original resting value due to the outflow of potassium ions.

During phase two, the membrane resistance R_m strongly decreases. The amount of open sodium channels is large and the netto ion-current is high. During this phase, which lasts around 0.5 – 1 ms, the tissue impedance at low frequencies decreases accordingly, since the membrane resistance no longer acts as an insulator. During the other phases, the drop of the membrane impedance due to open potassium and calcium channels is too small to exert a noticeable effect.

It is well known in electrophysiology that pacing amplitudes well above the threshold are linked to an upstroke that can be recognized from an immediate change of the characteristics of the pacing pulse. The voltage to current relationship changes during the pulse. With stimulus pulses close to the threshold, the action potential is

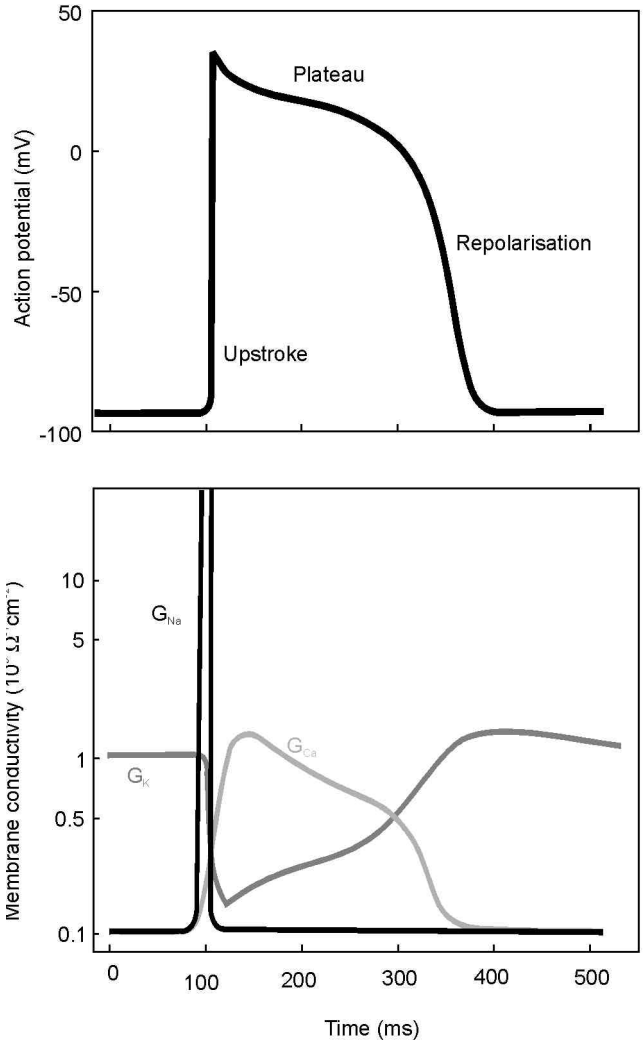

Figure 2. The transmembrane potential and the ionic conductivities of the membrane during the various phases of the action potential [13]. G_{Na}, G_K, and G_{Ca} are the membrane conductions for sodium, potassium, and calcium.

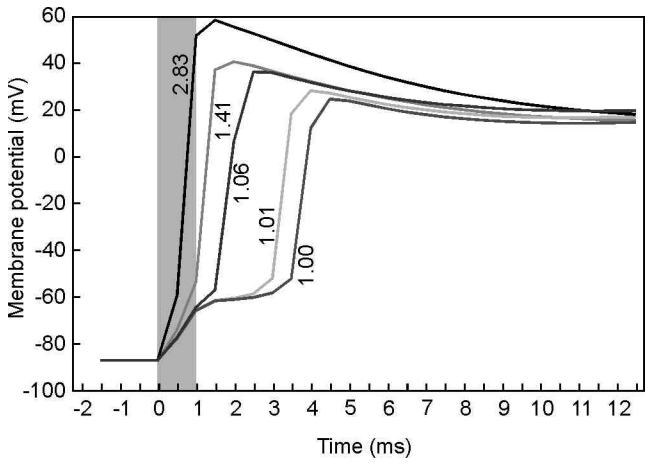

Figure 3. At pacing amplitudes close to the threshold, the action potential is delayed up to 4 ms after the pulse. Indices indicate the pacing amplitude normalized to the threshold value ($U_{pacing}/U_{threshold}$).

delayed. Simulations show that the upstroke of the potential is expected up to 4 ms after the pulse, so that any impedance dip will be outside the stimulus pulse (Figure 3).

Geometric Model of the Paced Event

During the experiments, geometric aspects further refined the model in order to fully understand the measurement results. In this geometric model the pacemaker electrode tip is placed inside a planar part of the ventricular wall. The excitable myocardium is separated from the blood by the thin (0.5 – 1 mm) non-excitable endocardium. There is a 1 mm sheath of fibrous tissue between the excitable tissue and electrode tip (Figure 4a). The conductivity of the blood is approximately 2 – 3 higher than that of the myocardium in a direction transverse to the muscle fibers. As a result, most of the pacing current and of the impedance measurement current "leaks" into the blood, so that current density inside the blood is higher than in the myocardium (at larger distances from the electrode tip). The electrode tip is an iso-potential boundary. Due to the so-called "edge-effect," current density is highest at the edges. Therefore, a substantial part of the current passes through the fibrous tissue and the endocardium directly into the blood without entering the myocardium.

Cathodal stimulation near the threshold level results in a stimulation of the myocardial cells adjacent to the electrode tip. The wavefront of the action potential spreads in an ellipsoidal manner; the velocity of the action potential is lower in a direction perpendicular to the muscle fibers. The longitudinal action potential velocity is approximately 50 cm/s The sodium in-current phase lasts approximately 0.5 – 1 ms. With a velocity of 50 cm/s, this constitutes a "slab" of sodium-active myocardium with a thickness of approximately 0.4 (range 0.25 – 0.5) mm. Initially, the increased conductivity of this sodium-active tissue is not reflected in the electrode impedance because the total volume of this tissue is very small. A more substantial influence will be seen at the very moment when the sodium-active tissue encompasses the myocardial tissue in the corner between the endocardium

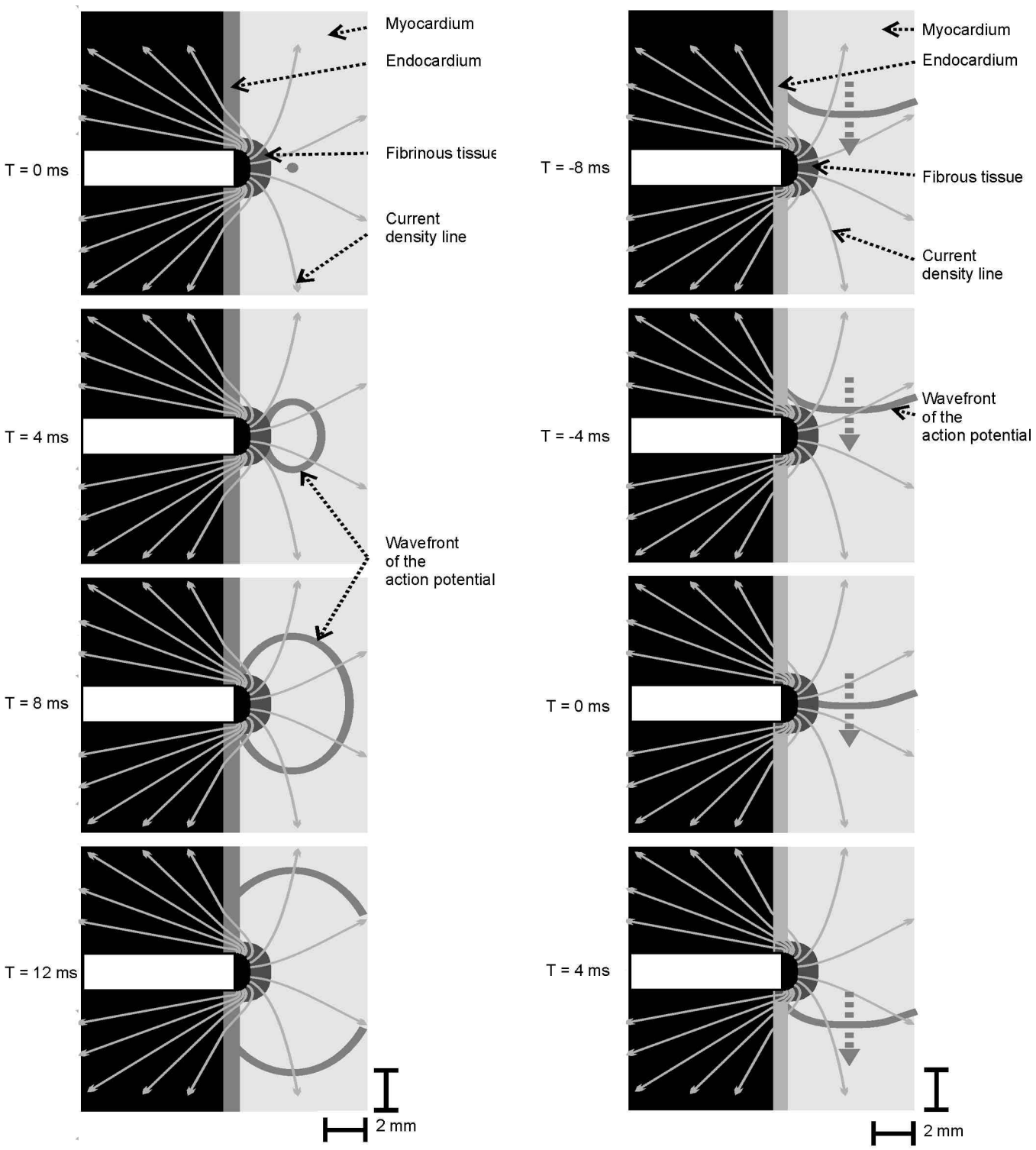

Figure 4. Expansion of the wavefront of a paced event at 0, 4, 8, and 12 ms after capture (panel a). The wavefront of an intrinsic event at -8, -4, 0, and 4 ms before/after passing the electrode tip (panel b).

and fibrous tissue (at T = 8 ms in the picture). Current densities in this area are high and the space angle of the active tissue with respect to the current source (electrode tip) is also substantial. While the action potential wavefront further expands the influence on the electrode tip, the impedance is diminished as the current density over the sodium-active slab decreases (lower field strength at a larger distance). Thus, the strongest impedance decrease is expected about 8 ms after initialization of the action potential. Adding a near-threshold delay of 4 ms (Figure 3) results in an impedance dip at around 12 ms after stimulus pulse. It is more difficult to predict the amplitude of the impedance dip from the model. The main factors involved are given below:

- The mere change in tissue impedance of the active myocardium is roughly estimated at 60 – 70% (f_1).
- Due to the thickness of the fibrous tissue layer, the sodium active slab never comprises the region with the highest current density. The minimum distance of sodium-active tissue to the electrode surface is approximately equal to the radius of the electrode R. The thickness of the slab of active tissue is approximately half of this radius. Given a 1/R dependence of the electrical potential (first-order estimation) in the close vicinity of the electrode tip and an electrode potential V_{el}, the potentials at both sides of the active slab are approximately $V_{el}/2$ and $V_{el}/2.4$, respectively. Thus, the slab in a non-active state adds approximately *1/2 - 1/2.4 = 0.08* of the total electrode impedance within a specific space angle (f_2).
- The space angle of the active myocardium in the high current density zone as seen by the electrode is relatively small compared to the total space angle. The sodium-active tissue in the corner between the endocardium and fibrous tissue constitutes a ring with a radius of 2R, and a thickness (in two directions) of approximately 0.4R. Therefore, the space angle with respect to the center of the electrode tip is approximately $(2p^* 2R)^*(0.4R)/(2R)^2 = 0.4pR$. The total space angle is $4\pi R$. Therefore, a reduction of approximately a factor of 10 is expected (f_3).
- The current density in the active zone is roughly estimated to be above average by approximately a factor of two (f_4).

Overall, the amplitude of the impedance dip with respect to the DC impedance of the unexcited tissue is expected to be approximately $f_1 * f_2 * f_3 / f_4 = 0.6 * 0.08 * 2 / 10 = 0.01 = 1\%$.

Geometric Model of the Sensed Event

The major difference with the paced model is the propagation pattern of the action potential. Instead of an ellipsoidal expanding wavefront, the action potential in the first approximation has a planar wavefront. (Note: From electrophysiology it is known that the wavefront is slightly curved at the boundary of the myocardium). The wavefront passes the electrode tip with a constant velocity of approximately 50 cm/s. The change in excitation propagation has some major consequences for the impedance dip. A substantial influence on the impedance is expected the very moment the wavefront reaches the boundary of the fibrous tissue. It lasts for approximately 6 – 8 ms before leaving the fibrous region at the other side of the electrode tip. Therefore, the impedance dip is broader than that of a paced event. However, at no time will the active front comprise the complete tissue in the corner between the endocardium and fibrous tissue. Only part of this high-current density will be involved at any moment. Therefore, the amplitude of the impedance dip is smaller than that of a paced event.

Materials and Methods

Five patients (four male; four with 1° AV block; one with sick sinus syndrome) implanted with an Inos² CLS

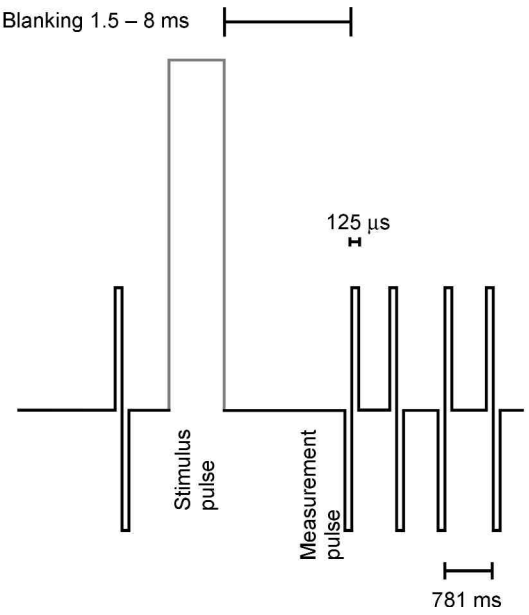

Figure 5. Time relationship between stimulus pulse and measurement pulses.

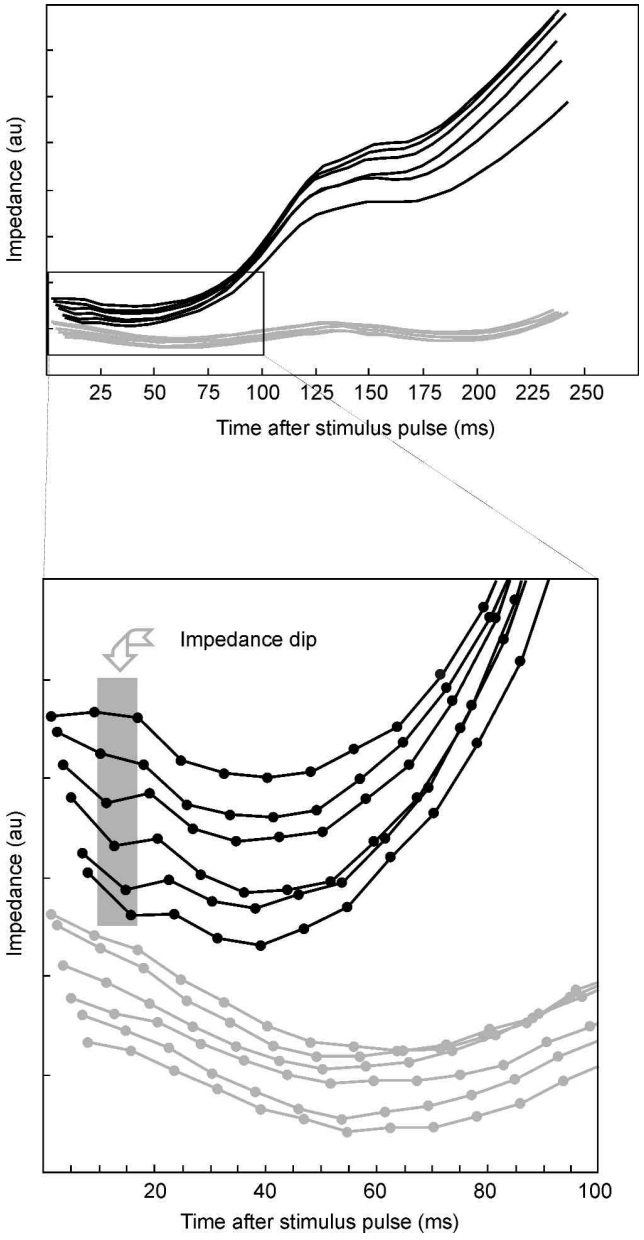

Figure 6. Impedance curves for one patient; au = arbitrary units. Each curve represents the average impedance curve measured for a specific pacing amplitude and at a specific measurement time-delay. The lower, flat curves are correlated to non-capture pulses. The upper curves represent capture-events; the impedance increase begins to occur approximately 50 ms after the stimulus pulse, when the ventricle starts to contract. The very beginning of the curves is further magnified in the second part of the figure. The impedance of the non-capture events occurs smoothly. However, the curves of the capture events show a small but distinct dip between 10 and 18 ms after the stimulus pulse.

pacemaker (Biotronik, Germany) and low polarization leads were paced in the DDD mode with a pacing rate slightly above the intrinsic rate. A short AV delay prevented fusions and pseudo-fusions. Just before the ventricular stimulus pulse, the bipolar ventricular impedance was measured with a sub-threshold, biphasic current pulse. After the pacing pulse, the waveform of the impedance was monitored with a series of 31 measurement pulses at a 128 Hz repetition rate (Figure 5).
The biphasic pulses had an amplitude of 212 μA and a phase duration of 125 μs. The time between the end of the stimulus and the first measuring pulse was shifted from 1.5 to 8 ms in five steps. Measurements were performed with two pacing amplitudes: at half the threshold and ~10% above the threshold value. Capture/non-capture was continuously monitored and recorded by an external ECG. Impedance data were downloaded via telemetry from the pacemaker into a programmer for post-processing.

Results

In all patients, a small (mean 2.9 ± 0.8 Ω) and fast (< 6 ms) dip in intracardiac impedance was detected 10 – 18 ms after ventricular capture (Figure 6). This dip was not observed during non-captured events. The mean value of intracardiac DC impedance was 542 ± 50 Ω.

Discussion

Preliminary clinical data seem to support the physiologic model in terms of amplitude and timing of the impedance dip. However, due to hardware limitations, the sampling interval for impedance measurement was too long for an exact determination of the shape and duration of the impedance dip. Further studies with better equipment are required to study these characteristics in greater detail. These studies should also be used to verify the impedance properties of intrinsic events, as well as at various locations (atrium, ventricle, outflow tract, …). Event detection by monitoring the sodium channels is not only very fast, it also has a number of other advantages compared to conventional method using the ventricular evoked response (VER) signal. Since a very local impedance measurement is used, there is no crosstalk and the method is not expected to be sensitive to RF interference. Also, fusion beats do not cause problems with the algorithm in the way seen in VER-based methods.

In principle, the method works for right/left atrial and left ventricular capture as well. Should non-capture occur, detection would be fast enough to allow delivery of a full energy back-up pulse. If this feature were implemented in a multisite pacemaker, it would preserve the patient's hemodynamic effect on cardiac resynchronization by assuring left ventricular capture at any time.

Conclusion

The preliminary results of this pilot study show that an ultra-fast (within 20 ms) detection of right ventricular capture is feasible by monitoring intracardiac impedance variations during the opening of the sodium channel. Since impedance measurement is slightly affected by polarization artifacts, such a method is expected to be effective with any lead. Dedicated hardware for a thorough analysis of the physiologic signal and a larger cohort of enrolled patients are needed in order to perform a significant statistical analysis.

References

[1] Sperzel J, Neuzner J, Schwarz T, et al. Reduction of pacing output coupling capacitance for sensing the evoked response. PACE. 2001; 24: 1377-1382.

[2] Kadhiresan VA, Olive A, Gornick C, et al. Automatic capture verification by charge-neutral sensing. PACE. 1999; 22: 73-78.

[3] Vonk BF, Van Oort G. New method of atrial and ventricular capture detection. PACE. 1998; 21 (Part 2): 217-222.

[4] Feld GK, Love CJ, Camerlo J, et al. A new pacemaker algorithm for continuous capture verification and automatic threshold determination: elimination of pacemaker afterpotential utilizing a triphasic charge balancing system. PACE. 1992; 15: 171-178.

[5] Curtis AB, Maas SM, Domijan A Jr, et al. A method for analysis of the local atrial evoked response for determination of atrial capture in permanent pacing systems. PACE. 1991; 14: 1576-1581.

[6] Livingston AR, Callaghan FJ, Byrd CL, et al. Atrial capture detection with endocardial electrodes. PACE. 1988; 11(Part 2): 1770-1776.

[7] Clarke M, Liu B, Schüller H, et al. Automatic adjustment of pacemaker stimulation output correlated with continuously monitored capture threshold: A multicenter study. PACE. 1998; 21: 1567-1575

[8] Schuchert A, Ventura R, Meinertz T, et al. Adjustment of the evoked response sensitivity after hospital discharge in pacemaker patients with automatic ventricular threshold tracking activated. PACE. 2001; 24: 212-216.

[9] Madrid AH, Olague J, Cercas A, et al. A prospective multicenter study on the safety of a pacemaker with automatic energy control: influence of the electrical factor on chronic stimulation threshold. PACE. Investigators. PACE. 2000; 23: 1359-1364.

[10] Schuchert A, Meinertz T. Uni- and bipolar pacing threshold measurements with capture control, a new automatic pacemaker function for capture verification. Comparison of the automatic and the manual pacing threshold measurement. Cardiology. 1999; 92: 210-213.

[11] Alt E, Kriegler E, Fituhi P, et al. Feasibility of using intracardiac impedance measurements for capture detection. PACE. 1992; 15: 1873-1879.

[12] Rigaud B, Hamzaoui L, Frikha MR, et al. In vitro tissue characterization and modelling using electrical impedance measurements in the 100 Hz – 10 MHz frequency range. Physiol Meas. 1995; 16: A15-A28.

[13] Schmidt RF, Thews G. Physiologie des Menschen. Berlin: Springer-Verlag. 2000: 472-497.

Contact
Antonio P. Ravazzi, MD
Divisione di Cardiologia Ospedale Civile SS
Antonio e Biagio
Via Venezia 18
15 100 Alessandria
Italy
Telephone: +39 0131 206297
Fax: +39 0131 206204
E-mail: ravazzim@tin.it